RHBDD2-WWOX protein interaction during proliferative and differentiated stages in normal and breast cancer cells

VALERIA ALEJANDRA FERRETTI[1], ROMINA CANZONERI[1], SABINA PALMA[1],
EZEQUIEL LACUNZA[1], CLAUDIO MARCELO ALDAZ[2] and MARTÍN CARLOS ABBA[1]

[1]Basic and Applied Immunological Research Center, School of Medical Sciences, National University of La Plata,
La Plata, Buenos Aires CP1900, Argentina; [2]Department of Epigenetics and Molecular Carcinogenesis,
The University of Texas M.D. Anderson Cancer Center, Science Park, Smithville, TX 78957, USA

Abstract. Rhomboid pseudoproteases are catalytically inactive members of the rhomboid superfamily that modulate the traffic, turnover and activity of their target proteins. Rhomboid domain containing 2 (*RHBDD2*) is a rhomboid family member overexpressed during mammary gland development and advanced stages of breast cancer. Interactome profiling studies have identified RHBDD2 as a novel binding partner of WW domain-containing oxidoreductase (WWOX) protein. The present study characterized the RHBDD2-WWOX interaction in proliferating and differentiated stages of normal mammary and breast cancer cells by co-immunoprecipitation and confocal microscopy. Normal breast and proliferating cancer cells showed significantly increased *RHBDD2* mRNA levels compared with their differentiated counterparts. *WWOX* mRNA was primarily expressed in differentiated cells. WWOX co-precipitated with RHBDD2, indicating that endogenous RHBDD2 and WWOX were physically associated in normal and breast cancer proliferating cells compared with the differentiated stage. Co-localization assays corroborated the co-immunoprecipitation results, demonstrating the RHBDD2-WWOX protein interaction in normal and proliferating breast cancer cells. RHBDD2 harbors a conserved LPPY motif at the C-terminus region that directly interacted with the WW domains of WWOX. Since WWOX serves as an inhibitor of the TGFβ/SMAD3 signaling pathway in breast cells, modulation of SMAD3 target genes was analyzed in proliferating and differentiated mammary cells and in *RHBDD2* silencing assays. Increased expression levels of SMAD3-regulated genes were detected in proliferating cells compared with their differentiated counterparts. Follistatin and angiopoietin-like 4 mRNA was significantly downregulated in *RHBDD2* transiently silenced cells compared with scrambled control small interfering RNA. Based on these results, WWOX was suggested to be a novel RHBDD2 target protein involved in the modulation of breast epithelial cell proliferation and differentiation.

Introduction

The rhomboid gene family encodes a heterogeneous group of polytopic proteins, with and without protease activity, which is conserved throughout evolution (1). A total of 14 human rhomboid-like proteins have been described, of which five are classified as active proteases [rhomboid-like 1 (RHBDL1), RHBDL2, RHBDL3, RHBDL4 and presenilin-associated rhomboid-like) and nine as pseudoproteases [inactive rhomboid proteins (iRhoms) 1-2, Derlins 1-3, UBA domain-containing 2 (UBAC2), rhomboid domain containing (RHBDD)2, RHBDD3 and transmembrane protein 115] (2). Rhomboid pseudoproteases lack catalytic activity and are primarily located in the endoplasmic reticulum (ER) and Golgi apparatus (3). The functional role of these pseudoproteases includes the ability to recognize and recruit target proteins to regulate their subcellular fate, turnover and degradation, affecting various signaling pathways and pathophysiological processes (2). A number of rhomboid pseudoproteases are associated with neoplastic disease (including iRhom1, iRhom2 and Derlin1) via activation of diverse cancer signaling pathways, such as WNT, HIF-1, VEGF and EGFR signaling (4-7).

Our previous studies determined that *RHBDD2* expression is increased in advanced stages of breast and colorectal cancer (8,9). Our subsequent study demonstrated that *RHBDD2* abrogation in breast cancer cell lines is associated with cell proliferation and modulation of the unfolded protein response pathway (10). Further analysis showed that increased *RHBDD2* expression is associated with the proliferative stages of mammary gland development (11), however, the mechanistic role of such upregulation remains to be determined. Recently, high-throughput proteomic approaches identified RHBDD2 as a novel putative interactor of WW domain-containing oxidoreductase (WWOX) (12). However, proteins that interact

Correspondence to: Dr Martín Carlos Abba, Basic and Applied Immunological Research Center, School of Medical Sciences, National University of La Plata, 60 and 120 Streets, La Plata, Buenos Aires 1900, Argentina
E-mail: mcabba@gmail.com

with RHBDD2 and their associated functions have not been defined yet in normal and breast cancer cells. WWOX has been described as a tumor suppressor that is frequently altered in breast cancer; its function is mediated by its interactions with cancer-associated proteins in luminal-like breast cancer cells (13). This ability to interact with multiple proteins is due to WW domains within its protein structure (14-16). For example, WWOX serves as an inhibitor of TGFβ signaling by binding to SMAD3 via its WW domains and modulating nuclear translocation of this transcription factor, thus decreasing promoter occupation and transcriptional activation (17). In addition, several studies using conditional ablation animal models have shown that WWOX serves an essential role in cell proliferation and differentiation during murine mammary gland development (17-20).

Given that RHBDD2 is a cancer-associated protein overexpressed in breast cancer cells that may be involved in protein trafficking, WWOX is a tumor suppressor involved in mammary cell proliferation and differentiation and RHBDD2 has been described as a putative interactor of WWOX, it was hypothesized that RHBDD2-WWOX protein interaction may serve as a negative regulator of WWOX tumor suppressor activity by their sequestering in the Golgi compartment. The present study aimed to to corroborate the RHBDD2-WWOX interaction and determine whether this affects proliferation and differentiation processes in normal mammary and breast cancer cells via modulation of the TGFβ signaling pathway.

Materials and methods

Cell lines, culture and differentiation. HC11 cells (proliferating cells) were grown at 37°C to subconfluence in RPMI-1640 (Gibco; Thermo Fisher Scientific, Inc.) supplemented with 10% FCS (Natocor) and 5 μg/ml insulin (Sigma-Aldrich; Merck KGaA). Then, confluent HC11 cells (competent cells) were maintained in RPMI-1640 with 2% FCS and 5 μg/ml insulin for 3 days, after which 5 μg/ml ovine prolactin (PRL; Sigma-Aldrich; Merck KGaA) was added for 3 days (differentiated cells). MCF7 and T47D breast cancer cells (proliferating PRL⁻ cells; American Type Culture Collection, Manassas, VA, USA) were grown to subconfluence in DMEM (Sigma-Aldrich; Merck KGaA) with 10% FCS at 37°C in a humidified atmosphere with 5% CO_2. T47D confluent cells were grown at 37°C and treated with PRL (3 μg/ml) in DMEM with 2% FCS for 3 days.

Subcellular fractions. HC11 and T47D cells were grown at 37°C in 10-cm plastic dishes until subconfluence, harvested by trypsinization and then washed 3 times with cold PBS at 300 x g for 5 min at 4°C. The cells were subsequently incubated at 4°C with 2 ml 10 mM HEPES (pH, 7.9; Sigma-Aldrich; Merck KGaA), 150 mM NaCl (Merck KGaA), 50 mM Tris-HCl (Merck KGaA), 1 mM PMSF and 1% NP-40 buffer supplemented with protease inhibitor cocktail (both Sigma-Aldrich; Merck KGaA). Cells were transferred to a dounce homogenizer (Sigma-Aldrich; Merck KgaA) and 10 strokes were applied while cell lysis was verified under a phase-contrast microscope at x10 magnification. Homogenized cells were centrifuged at 300 x g for 5 min at 4°C to obtain supernatant (cytoplasmic and membrane fraction) and pellet (nuclear fraction). Supernatant was ultracentrifuged at 100,000 x g for 45 min at 4°C using an ultracentrifuge (Beckman Coulter, Inc.; cat. no. LE-80K) to obtain the corresponding cytoplasmic and membrane fractions. Protein concentration was measured by Bradford assay (Bio-Rad Laboratories, Inc.) and samples were stored at -70°C.

Small interfering (si)RNA assay. MCF7 and T47D cell lines were cultured at 37°C on 12-well plates to 60% confluence in Opti-MEM I Reduced Serum Medium (Gibco; Thermo Fisher Scientific, Inc.) and transiently transfected with 40 pmol/μl siRNA mixed with Lipofectamine® according to the manufacturer's protocol (Invitrogen; Thermo Fisher Scientific, Inc.). siRNA (length, 21 nucleotides) against *RHBDD2* mRNA (RHBDD2-siRNA, 5'-CUGUGUUGGGUA CUUUGAUdTdT-3') was used as previously described (8). In addition, AccuTarget™ biotin-labeled negative control siRNA (5'-CCUACGCCACCAAUUUCGUdTdT-3'; Bioneer Corporation), which exhibits no homology to any human genome sequence, was used as a control. Cells were incubated at 37°C for 72 h.

RNA isolation and reverse transcription-quantitative (RT-q) PCR. Total RNA was isolated from HC11, MCF7 and T47D cell lines using TRIzol™ solution (Thermo Fisher Scientific, Inc.) according to manufacturer's instructions. RNA was reverse transcribed to cDNA using the SuperScript™ Reverse Transcriptase kit (Thermo Fisher Scientific, Inc.) according to the manufacturer's instructions. RT-qPCR was performed using PerfeCTa SYBR-Green SuperMix (Quantabio); primer sets are listed in Table SI. PCR conditions were as follows: Initial denaturation at 95°C for 3 min and 40 cycles of denaturation (95°C 40 sec), annealing (55°C, 30 sec) and extension (72°C, 30 sec). Data were captured and analyzed using the Agilent AriaMx Real-Time PCR System 1.5 software (Agilent Technologies, Inc.). Gene expression levels were calculated as $2^{-\Delta\Delta Cq}$ values using the housekeeping gene RNA18S as a reference (21).

Antibodies (Abs). The primary Abs were as follows: Rabbit anti-RHBDD2 (cat. no. TA306891; OriGene Technologies, Inc.), rabbit anti-WWOX (Aldaz Lab) (20), mouse anti-WWOX (cat. no. sc-374449; Santa Cruz Biotechnology, Inc.), mouse anti-human β-casein (cat. no. cat. no. sc-53189; Santa Cruz Biotechnology, Inc.), mouse anti-mouse β-casein (cat. no. sc-166520; Santa Cruz Biotechnology, Inc.) and mouse anti-follistatin (FST; cat. no. sc-365003; Santa Cruz Biotechnology, Inc.). Secondary Ab were as follows: Goat anti-rabbit IgG (Sigma-Aldrich; Merck KGaA), donkey anti-rabbit IgG Cy3-conjugated (cat. no. 711165152; Jackson ImmunoResearch Laboratories, Inc.), goat anti-mouse IgG biotinylated (cat. no. BA9200; Vector Laboratories, Inc.; Maravai LifeSciences) and anti-mouse IgG BP-CFL 488 (Santa Cruz Biotechnology, Inc.).

Co-immunoprecipitation (Co-IP). The cells were lysed with lysis buffer (50 nM Tris-HCl, pH, 7.4; 150 mM NaCl; 2 mM PMSF; and 1% NP-40). RHBDD2 and WWOX protein were immunoprecipitated from cell lysates. In order to obtain RHBDD2 and WWOX immune complexes, 300 μl homogenate

was incubated overnight with 5 µl Ab at 4°C (1:60). The immune complexes were isolated with protein A Sepharose CL-4B, which had been washed with cold lysis buffer followed by centrifugation at 10,000 x g for 30 sec at 4°C. A total of 300 µl lysates precipitated with corresponding Ab (containing the immune complexes) were incubated with 50 µl protein A Sepharose-CL-4B (Sigma-Aldrich; Merck KGaA; cat no GE17-0963-02) for 1 h on a rocking platform at 4°C and centrifuged at 10,000 x g for 30 sec at 4°C. The pellets were washed 5 times with 500 µl lysis buffer. In order to release the immune complexes, pellets were boiled for 10 min in Laemmli's buffer followed by centrifugation at 10,000 x g for 5 min at 4°C. The supernatants containing the isolated and purified immune complexes were analyzed by SDS-PAGE followed by western blot analysis.

SDS-PAGE and western blot analysis. The aforementioned cell lysates and immune complexes were diluted in 25% SDS, 10% glycerol and 2-mercaptoethanol (2:1), heated at 90°C for 5 min and separated in discontinuous 4-12, 5% acrylamide mini-gels. The protein concentration was measured by the Bradford method and 50 µg protein was loaded per lane. Following electrophoresis, gels were blotted onto nitrocellulose transfer membranes (Whatman plc; Cytiva) in wet conditions. Membranes were blocked with 3% powdered milk in 0.05% PBS/Tween-20 at 4°C overnight and washed in 0.05% PBS/Tween-20. Membranes were incubated primary Ab (anti-RHBDD2, 1:1,000; anti-WWOX, 1:2,000) at 4°C overnight. Following washing, membranes were incubated with the appropriate secondary Ab and protein bands were visualized by chemiluminescence on radiographic plates using the EasySee Western Blot kit (cat. no. DW101-01, TransGen Biotech Co., Ltd.). Loading controls such as ACTB and GAPDH were not included in the IP assays because they were not detected in the specifics immunoprecipitated.

Immunofluorescence and confocal microscopy. In order to evaluate the subcellular localization of RHBDD2, WWOX and FST protein, fluorescence immunohistochemistry analysis of proliferating HC11 and T47D cells was performed. Cells were grown at 37°C on 100 mm² cover glass to 70% confluence (or 100% in differentiated cells) and fixed for 1 h. with 4% formaldehyde at room temperature or cold acetone (100%). The cell membrane was permeabilized with 0.01% Triton for 10 min at room temperature. Then, cells were incubated overnight with primary Ab (anti-RHBDD2, 1:150; anti-WWOX, 1:150; anti-FST, 1:50) at 4°C. Cells were incubated for 2 h with the appropriate secondary Ab at room temperature, and nuclei were stained with propidium iodide (1:100) or DAPI for 1 h at room temperature. Finally, cells were visualized under an immunofluorescence microscope at 10 and 40x magnifications, and images were captured by Micrometrics SE Premium 4.5 software (Unitron Ltd.). Then, RHBDD2 and WWOX co-localization was viewed under a confocal immunofluorescence microscope at x10 and x40 magnifications (Confocal FluoView™ 1000) and images were acquired at red and green signal channels using FluoView FV1000 software (Olympus Latin America, Inc.). Co-localization analysis was performed with the JaCoP application on ImageJ software 1.8.0 (National Institutes of Health). Mander's overlap coefficient (MOC) was used to quantify the degree of co-localization between fluorophores. Pearson's correlation coefficient was calculated between the mean intensity values of the overlapping green (WWOX localization) and red signals (RHBDD2 localization).

In silico analysis of RHBDD2 and WWOX expression in normal and breast cancer cells. In order to evaluate the relevance of the combined *RHBDD2* and *WWOX* mRNA expression between normal tissue and primary breast carcinoma, The Cancer Genome Atlas (TCGA)-BRCA dataset was analyzed. Briefly, *RHBDD2* and *WWOX* expression profiles from 1,211 breast samples (114 normal and 1,097 tumor samples) and their intrinsic subtypes were retrieved from the University of California Santa Cruz Xena browser (xena.ucsc. edu/). Primary invasive breast carcinoma was classified as low or high WWOX mRNA expression according to the median expression value (7.85) of the normalized profile. *In silico* prediction of RHBDD2 protein structure was performed with PROTTER 1.0 software (wlab.ethz.ch/protter/start/).

Statistical analysis. Data are presented as the mean ± SEM (measured in triplicate). Kolmogorov-Smirnov and Shapiro-Wilk tests were used to evaluate the distribution of the obtained data. RT-qPCR data analysis was performed using Mann-Whitney U test in R software 3.6.2 (r-project.org/). *RHBDD2* and *WWOX* expression levels from *in silico* analysis were using Mann-Whitney U test. P<0.05 was considered to indicate a statistically significant difference.

Results

RHBDD2 and WWOX mRNAs are differentially modulated in differentiated and proliferating human and mouse mammary cells. Expression of both RHBDD2 and WWOX transcripts in normal and breast cancer cell lines was evaluated by RT-qPCR. The highest levels of *RHBDD2* expression were observed in T47D breast cancer cell line, while *WWOX* mRNA was highly expressed in MCF7 breast cancer cells (Fig. 1A). HC11 and T47D proliferative cells showed significantly increased *RHBDD2* expression levels compared with differentiated or PRL-treated counterparts (P<0.05; Fig. 1B). *WWOX* was highly expressed in differentiated HC11 and PRL-treated T47D cells compared with the proliferating and PRL⁻ cells, respectively (P<0.05; Fig. 1B). PRL-induced differentiation was confirmed by elevated β-casein expression in differentiated cells compared with proliferating cells (Fig. 1B).

RHBDD2-WWOX interaction increases in proliferative normal and breast cancer cells. In order to investigate whether RHBDD2 and WWOX proteins physically interact, co-IP was investigated in normal mammary and breast cancer cell models. Both proteins were co-immunoprecipitated in HC11 and MCF7 whole cell lysates using anti-WWOX and anti-RHBDD2 Ab (Figs. 2A and S1). In order to evaluate whether the interaction between the aforementioned proteins was modulated by differentiation, co-IP analysis of differentiated and proliferative HC11 cells was performed. RHBDD2-WWOX IP was more abundant in proliferating
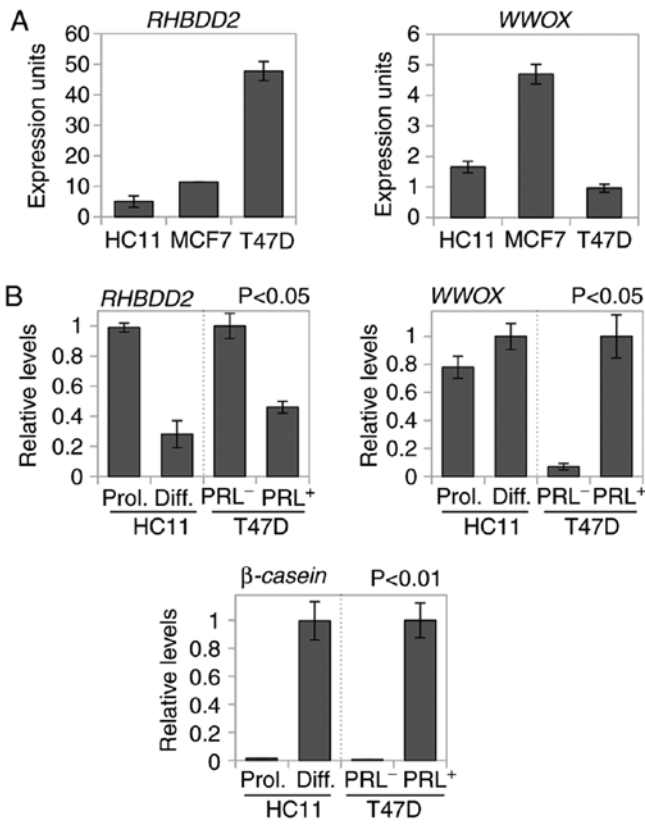
Figure 1. *RHBDD2* and *WWOX* expression analysis in normal and breast cancer cells. (A) RT-qPCR analysis of *RHBDD2* and *WWOX* in HC11 normal mammary cells and MCF7 and T47D breast cancer cell lines. Expression levels were normalized to RNA18S. (B) RT-qPCR analysis of *RHBDD2*, *WWOX* and *β-Casein* (differentiation marker) in proliferative and differentiated HC11 and T47D cells following lactogenic hormone stimulation (PRL⁺). Relative expression levels were normalized to Prol. (*RHBDD2*) or Diff. (*WWOX* and *β-Casein*) HC11 and T47D cells. RHBDD2, rhomboid domain containing 2; WWOX, WW domain-containing oxidoreductase; RT-q, reverse transcription-quantitative; PRL, prolactin; Prol., proliferative; Diff., differentiated.

Figure 2. RHBDD2 and WWOX co-IP analysis in normal mammary and breast cancer cell lines. (A) Co-IP of endogenous WWOX and RHBDD2 from HC11 and MCF7 cells. Whole-cell lysates were immunoprecipitated with anti-RHBDD2 Ab and immunoblotted with anti-WWOX Ab or immunoprecipitated with anti-WWOX Ab and immunoblotted with anti-RHBDD2 Ab. In both IP assays, non-primary Ab Ctrl and IP washes with unbound protein (washed 1 and 2) were included as non-specific Ctrls. (B) Co-IP of endogenous WWOX and RHBDD2 from HC11 Prol and Diff cells. Whole-cell fraction lysates were immunoprecipitated with anti-WWOX and immunoblotted with anti-RHBDD2 Ab. (C) Co-IP of endogenous WWOX and RHBDD2 from CF and MF derived from Prol., PRL⁻, Diff. or PRL⁺ HC11 and T47D cells. (D) RHBDD2 protein structure prediction using PROTTER software. A conserved LPPY amino acid sequence was identified in the carboxyl-terminal region (dark grey) of RHBDD2 protein. RHBDD2, rhomboid domain containing 2; WWOX, WW domain-containing oxidoreductase; IP, immunoprecipitation; PRL, prolactin; Prol., proliferative; Diff., differentiated; Ab, antibody; Ctrl, control; CF, cytoplasmic fraction; MF, membrane fraction.

HC11 mammary cells compared with differentiating cells (Fig. 2B), which may have been due to *RHBDD2* upregulation in the proliferating cells (Fig. 1B). Subcellular fractions from proliferative, differentiated or PRL-treated HC11 and T47D cells were co-immunoprecipitated with anti-WWOX Ab and immunoblotted with anti-RHBDD2 Ab. Strong co-expression of both proteins was detected in the membrane fractions of proliferating cells in both cell lines compared with the cytoplasmic fractions (Fig. 2C). HC11 differentiated and T47D PRL-treated cells showed lower co-expression in both subcellular fractions than their respective proliferative and PRL⁻ counterparts (Fig. 2C).

The ability of WWOX protein to ubiquitously interact with multiple proteins is attributed to the presence of two WW domains. WW domains are small protein modules that bind to proline-rich ligand consensus motifs, such as PPXY and LPXY (14-16). In order to predict RHBDD2 protein structure *in silico*, PROTTER software was used. *In silico* analysis of the RHBDD2 primary sequence suggested that it is an integral and polytopic protein containing 5 transmembrane domains and a proline-rich region (PRR) in the C-terminus (Fig. 2D). RHBDD2 harbored a conserved LPPY motif located

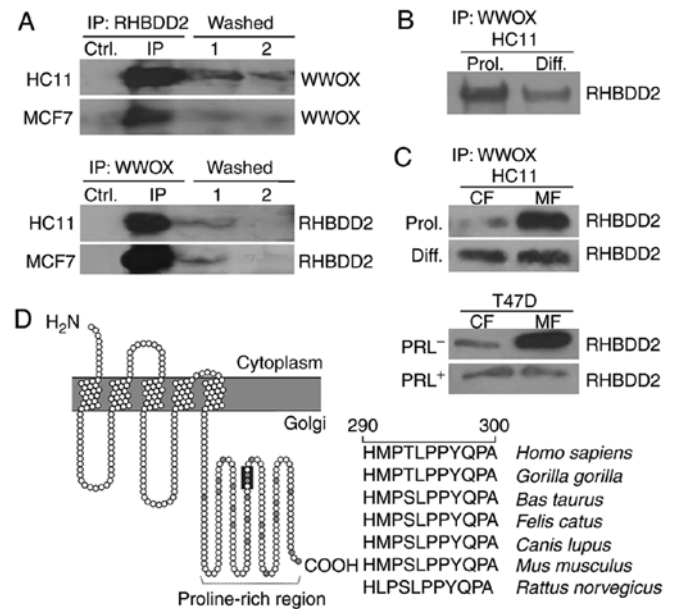in the PRR that directly interacted with the WW domains of WWOX. This LPPY motif is phylogenetically conserved across different species (Fig. 2D). Next, localization of the endogenous RHBDD2-WWOX complex was analyzed in proliferating HC11 and T47D proliferating; observed juxtanuclear co-localization of both proteins was observed (Fig. 3). Mander's test showed significant WWOX-RHBDD2 co-localization coefficients in both proliferating cell lines (MOC=0.99).

RHBDD2 modulates the TGFβ signaling pathway by interacting with WWOX. In order to determine whether RHBDD2-WWOX protein interaction was associated with modulation of the TGFβ/SMAD3 pathway during differentiation and/or proliferation of mammary cells, expression levels of two SMAD3 target genes [*FST* and angiopoietin-like 4 (*ANGPTL4*)] were evaluated in T47D cells. Increased *FST* and *ANGPTL4* mRNA expression levels were detected in T47D proliferating PRL⁻ cells compared with PRL-treated counterparts (P<0.01; Fig. 4A). FST upregulation in T47D proliferating cells was corroborated by immunofluorescence (Fig. 4B).

Furthermore, the effects of *RHBDD2* silencing on modulation of these TGFβ/SMAD3 target genes were evaluated in breast cancer cells with elevated endogenous *RHBDD2*
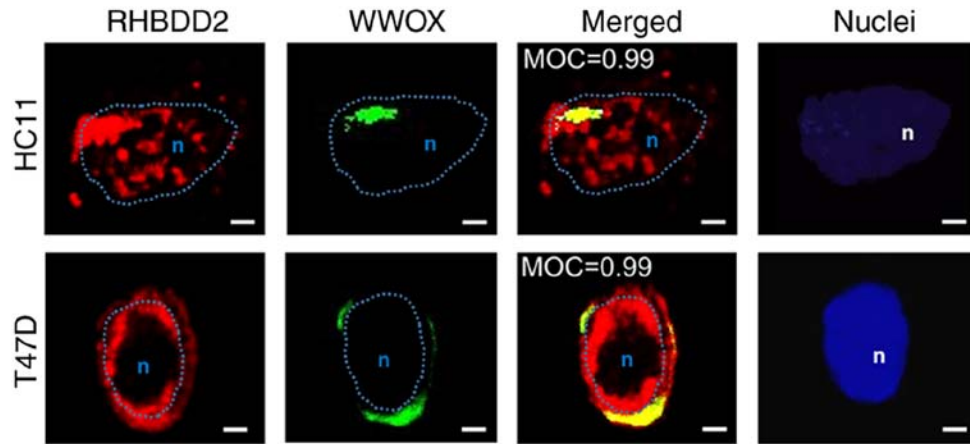
Figure 3. Confocal immunofluorescent analysis of RHBDD2 and WWOX in proliferating normal mammary and breast cancer cells. MOC was used to quantify the degree of co-localization between green (WWOX) and red signal (RHBDD2) in proliferating HC11 and T47D cells. Yellow, co-localization of both proteins; blue, DAPI. Scale bar, 10 μm. RHBDD2, rhomboid domain containing 2; WWOX, WW domain-containing oxidoreductase; MOC, Mander's overlap coefficient; n, nucleus.
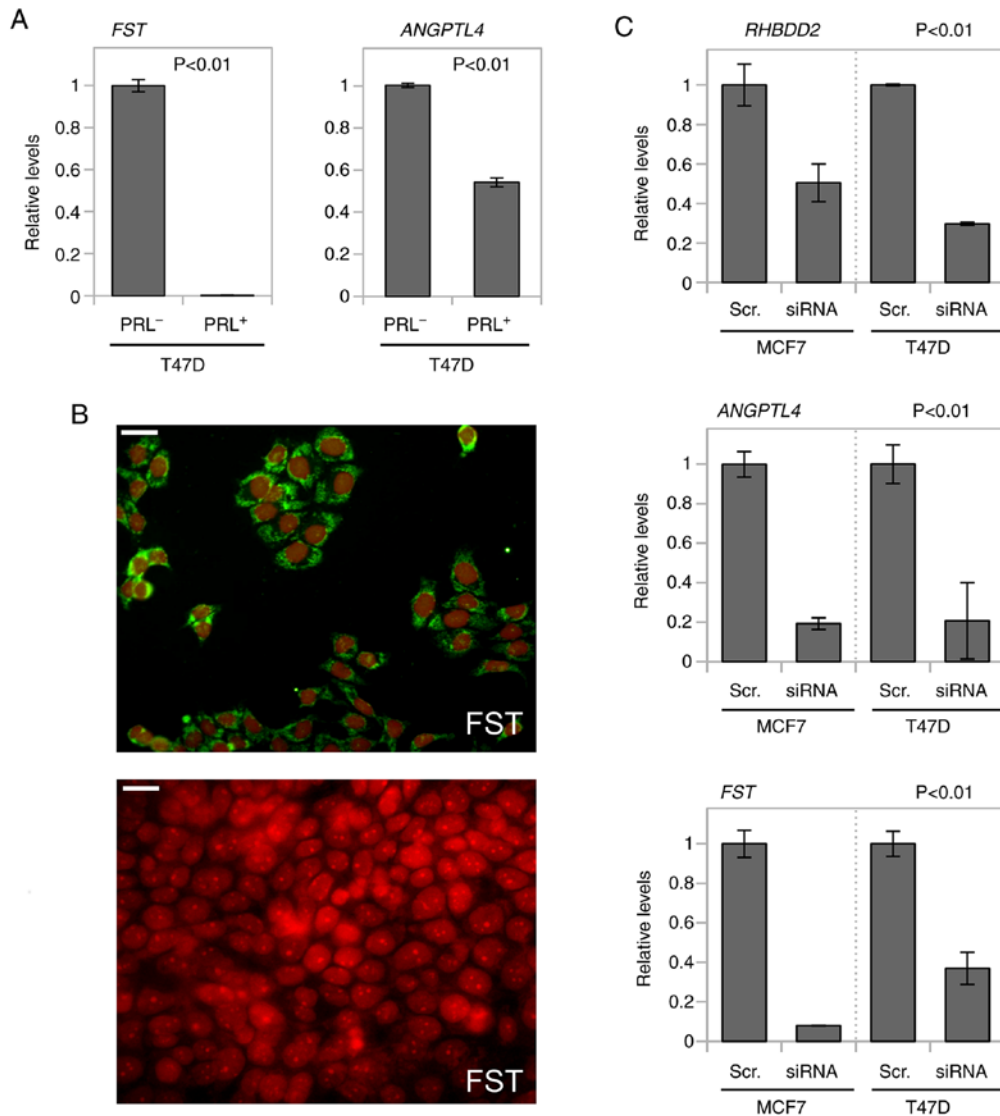

Figure 4. Expression level analysis of SMAD3 target genes in breast cancer cell lines. (A) RT-qPCR analysis of *FST* and *ANGPTL4* mRNA in T47D proliferating (PRL$^-$) and PRL$^+$ cells. Relative expression levels were normalized to proliferating cells. (B) Immunofluorescence analysis of FST protein (green) in T47D proliferating and PRL$^-$ cells. Red, nuclei stained with propidium iodide. Scale bar, 50 μm. (C) RT-qPCR analysis of *FST* and *ANGPTL4* expression in MCF7 and T47D *RHBDD2* silenced cells. Relative expression levels were normalized to Scr. RHBDD2, rhomboid domain containing 2; RT-q, reverse transcription-quantitative; FST, follistatin; ANGPTL4, angiopoietin-like 4; PRL, prolactin; Scr., scramble; si, small interfering.
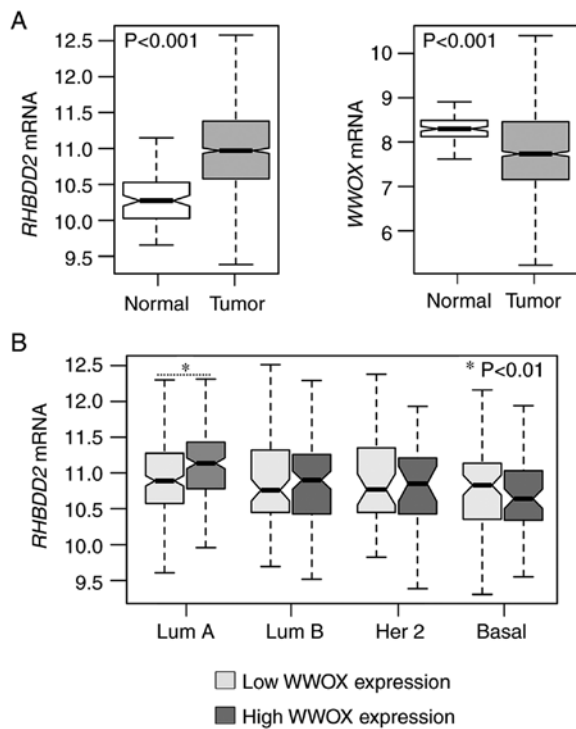
Figure 5. *In silico* analysis of *RHBDD2* and *WWOX* mRNA in normal and primary breast carcinoma obtained from The Cancer Genome Atlas-BRCA dataset. (A) Comparative analysis of *RHBDD2* and *WWOX* expression levels among normal (n=114) and primary invasive carcinoma (n=1,097) samples. (B) Comparative analysis of *RHBDD2* expression between high and low WWOX-expressing tumors according to intrinsic subtype. RHBDD2, rhomboid domain containing 2; WWOX, WW domain-containing oxidoreductase; lum, luminal; Her2, human epidermal growth factor receptor 2.

expression. A siRNA-mediated approach was used to transiently induce *RHBDD2* gene expression abrogation in MCF7 and T47D cells (Fig. 4C). *FST* and *ANGPTL4* mRNA was significantly downregulated in *RHBDD2*-silenced cells compared with scrambled control siRNA (P<0.01; Fig. 4C).

RHBDD2 overexpression in luminal A breast cancer with high WWOX expression. *RHBDD2* and *WWOX* mRNA expression was evaluated in normal and breast cancer samples obtained from the TCGA-BRCA project (n=1,211). Primary invasive breast carcinoma showed consistent upregulation of *RHBDD2* and downregulation of *WWOX* (both P<0.001) compared with normal samples (Fig. 5A). In order to assess whether *RHBDD2* overexpression was associated with *WWOX* expression levels, WWOX mRNA profiles were classified as low- or high-expression according to each intrinsic subtype. *RHBDD2* expression was significantly upregulated in luminal A breast carcinoma, which was the intrinsic subgroup with the highest *WWOX* expression levels (P<0.01; Fig. 5B).

Discussion

Our previous studies determined that the *RHBDD2* gene is overexpressed in advanced stages of breast and colorectal cancer, suggesting a role in tumor progression and chemo-resistance to neoadjuvant therapy (8,9,22). Under normal physiological conditions, RHBDD2 expression is detected not only in embryonic and developing rat tissue but also in

proliferating adult rat tissue (11). Regarding the mammary gland, increased Rhbdd2 expression is associated with the pregnancy stage (11). *RHBDD2* encodes one of nine known rhomboid pseudoproteases whose functional roles are defined by binding to target proteins (2). Recently, RHBDD2 was detected among multiple WWOX protein interactors under physiological conditions using a proteomic scale approach (12). The present study evaluated the expression levels and interaction between RHBDD2 and WWOX in proliferating and differentiated normal mammary and breast cancer cells to define the mechanistic role of RHBDD2.

RHBDD2 and *WWOX* mRNA expression levels were detected in both luminal-like breast cancer cell lines (MCF7 and T47D). MCF7 is the breast cancer cell line with the highest *WWOX* mRNA expression levels and is characterized by its high dependence on estradiol for growth (23). Here, two PRL-responsive mammary epithelial cell lines (HC11 and T47D) were used to analyze *RHBDD2* and *WWOX* expression levels and protein interaction in differentiated and proliferating cells. HC11 mouse mammary epithelial cells were used as a normal differentiation model due to their ability to produce β-casein under lactogenic hormone stimulation and to produce extracellular matrix during differentiation (24). HC11 cells only produce β-casein when lactogenic hormones are added to confluent cells, not to proliferating HC11 cells (24). T47D luminal-like breast cancer cells can be induced either to proliferate or differentiate; following under PRL stimulation, these cells underwent differentiation, which is characterized by morphological changes, production of lipid vesicles and expression of β-casein (25-27). Proliferating normal and breast cancer proliferating showed significantly increased *RHBDD2* mRNA levels compared with their differentiated counterparts. *WWOX* mRNA was primarily expressed in differentiated cells. These results were consistent with previous studies in rat mammary gland development and human breast cancer cells, indicating that *RHBDD2* is highly expressed in proliferating cells (10,11,28). Co-IP suggested that RHBDD2-WWOX protein interaction primarily occured in the membrane fraction of proliferating cells and decreased in differentiated cells. Immunodetection of both proteins in the membrane-enriched fraction was consistent with previous studies that demonstrated that WWOX and RHBDD2 are localized to perinuclear regions overlapping the Golgi compartment (20,28). The co-localization results corroborated co-IP data suggesting RHBDD2 and WWOX interacting proteins reside, at least transiently, in the same cellular compartment of proliferating cells. Moreover, physical interaction between both proteins was supported by identification of a conserved LPPY motif at the C-terminus region of RHBDD2 that directly interact with the WW domains of WWOX.

Human WWOX primarily localizes to juxtanuclear regions significantly overlapping Golgi compartment (20); here, RHBDD2 displayed a vesicular distribution consistent with endosomal compartmentalization. Our previous studies demonstrated that RHBDD2 protein is primarily located in the Golgi apparatus of HC11, MCF7 and T47D cells (11,28) is and associated with vesicle SNAP receptor transport vesicles, suggesting a putative role in protein trafficking (28). Among the known WWOX interactors, several proteins are associated

with protein trafficking from ER exit sites to Golgi and from late endosomes to lysosomes, such as SEC23-interacting protein, secretory carrier membrane protein 3 and vesicular, overexpressed in cancer, pro-survival protein 1 (*VOPP1*) (12). Furthermore, Bonin *et al* (29) reported that VOPP1 physically interacts with WWOX and that upon binding, WWOX translocates to the VOPP1-containing lysosomal compartment, serving as a negative regulator of WWOX tumor suppressor activity. WWOX expression loss is common in various types of cancer and is implicated in normal mammary gland proliferation and differentiation processes. Our previous study reported that WWOX modulates the TGFβ signaling pathway in normal breast cells by binding and sequestering SMAD3 in the cytoplasmic compartment (17). In order to investigate the role of RHBDD2-WWOX protein interaction in the modulation of the TGFβ/SMAD3 pathway, expression of SMAD3 target genes was evaluated in proliferating and differentiated T47D cells and following transient *RHBDD2* abrogation. Increased gene expression levels of *FST* and *ANGPTL4* were detected in proliferating T47D cells compared with their differentiated counterparts. In addition, *FST* and *ANGPTL4* mRNA was significantly downregulated in *RHBDD2* transiently silenced cells. High *FST* and *ANGPTL4* expression suggested that the TGFβ/SMAD3 signaling pathway was active in proliferating T47D cells and *RHBDD2* depletion in luminal-like breast cancer cells may affect cell proliferation by modulating TGFB/SMAD3 signaling via WWOX interactions.

It was hypothesized that *RHBDD2* expression may contribute to unfavorable clinical breast cancer outcome due to its inhibitory effect on *WWOX* tumor suppressor activity. Luminal breast cancer is an intrinsic subtype characterized by tumors that are predominantly regulated by estrogen receptors and respond to endocrine therapy (30). In addition, WWOX expression positively correlates with expression levels of hormone receptors and its expression is significantly decreased or lost in ER⁻ breast cancer (31). The present results showed a consistent upregulation of *RHBDD2* and downregulation of *WWOX* in primary invasive breast carcinoma compared with normal samples. *RHBDD2* expression was significantly upregulated in luminal A primary invasive breast carcinoma, which is the intrinsic subtype with the highest *WWOX* expression levels. These data suggest that *RHBDD2* overexpression may influence breast cancer progression in luminal A tumors with WWOX expression favoring their interaction. The most common mechanism leading to loss of WWOX expression is genomic loss via gross chromosomal deletions and rearrangements (13). Mechanisms involving epigenetic silencing by promoter hypermethylation and degradation have also been described (13). The present findings identified post-translational sequestration of WWOX by RHBDD2 as an alternative mechanism underlying inhibition of the tumor-suppressive properties of WWOX.

In summary, the present results indicated that RHBDD2 interacted with WWOX protein; this interaction may serve a role in the TGFβ/SMAD3 signaling pathway, thus impacting the proliferation and differentiation of normal and neoplastic mammary epithelial cells. RHBDD2 overexpression in advanced breast cancer may promote the TGFβ/SMAD3 signaling pathway by sequestering WWOX in the Golgi apparatus or other membrane vesicles. RHBDD2-WWOX interaction promoted activation of SMAD3 target genes involved in mammary cell proliferation and breast cancer progression, promoting the development of luminal A breast carcinoma.

Availability of data and materials

The datasets used and/or analyzed during the current study are available from the corresponding author on reasonable request.

Authors' contributions

MCA and VAF conceptualized the study and designed the experiments. Experiments were performed by VAF, RC and SP. MCA and EL performed statistical and bioinformatic analysis. MCA, VFA and CMA wrote the manuscript. MCA and VAF confirm the authenticity of all the raw data. All authors read and approved the final version of the manuscript.

Ethics approval and consent to participate

Not applicable.

Patient consent for publication

Not applicable.

Competing interests

The authors declare that they have no competing interests.

References

1. Freeman M: Rhomboid proteases and their biological functions. Annu Rev Genet 42: 191-210, 2008.
2. Adrain C and Cavadas M: The complex life of rhomboid pseudo-proteases. FEBS J 287: 4261-4283, 2020.
3. Bergbold N and Lemberg MK: Emerging role of rhomboid family proteins in mammalian biology and disease. Biochim Biophys Acta 1828: 2840-2848, 2013.
4. Yan Z, Zou H, Tian F, Grandis JR, Mixson AJ, Lu PY and Li LY: Human rhomboid family-1 gene silencing causes apoptosis or autophagy to epithelial cancer cells and inhibits xenograft tumor growth. Mol Cancer Ther 7: 1355-1364, 2008.
5. Zou H, Thomas SM, Yan Z, Grandis JR, Vogt A and Li L: Human rhomboid family-1 gene RHBDF1 participates in GPCR-mediated transactivation of EGFR growth signals in head and neck squamous cancer cells. FASEB J 23: 425-432, 2009.

6. Zhou Z, Liu F, Zhang ZS, Shu F, Zheng Y, Fu L and Li LY: Human rhomboid family-1 suppresses oxygen-independent degradation of hypoxia-inducible factor-1α in breast cancer. Cancer Res 74: 2719-2730, 2014.

7. Yuan H, Wei R, Xiao Y, Song Y, Wang J, Yu H, Fang T, Xu W and Mao S: RHBDF1 regulates APC-mediated stimulation of the epithelial-to-mesenchymal transition and proliferation of colorectal cancer cells in part via the Wnt/β-catenin signalling pathway. Exp Cell Res 368: 24-36, 2018.

8. Abba MC, Lacunza E, Nunez MI, Colussi A, Isla-Larrain M, Segal-Eiras A, Croce MV and Aldaz CM: Rhomboid domain containing 2 (RHBDD2): A novel cancer-related gene over-expressed in breast cancer. Biochim Biophys Acta 1792: 988-997, 2009.

9. Lacunza E, Canzoneri R, Rabassa ME, Zwenger A, Segal-Eiras A, Croce MV and Abba MC: RHBDD2: A 5-fluorouracil responsive gene overexpressed in the advanced stages of colorectal cancer. Tumour Biol 33: 2393-2399, 2012.

10. Lacunza E, Rabassa ME, Canzoneri R, Pellon-Maison M, Croce MV, Aldaz CM and Abba MC: Identification of signaling pathways modulated by RHBDD2 in breast cancer cells: A link to the unfolded protein response. Cell Stress Chaperones 19: 379-388, 2014.

11. Ferretti VA, Canzoneri R, Barbeito CG, Croce MV, Abba MC and Lacunza E: Spatiotemporal expression of rhomboid domain containing 2 (Rhbdd2) during rat development. Acta Histochem 117: 635-641, 2015.

12. Hussain T, Lee J, Abba MC, Chen J and Aldaz CM: Delineating WWOX protein interactome by tandem affinity purification-mass spectrometry: Identification of top interactors and key metabolic pathways involved. Front Oncol 8: 591, 2018.

13. Aldaz CM, Ferguson BW and Abba MC: WWOX at the crossroads of cancer, metabolic syndrome related traits and CNS pathologies. Biochim Biophys Acta 1846: 188-200, 2014.

14. Sudol M: Structure and function of the WW domain. Prog Biophys Mol Biol 65: 113-132, 1996.

15. Chan DC, Bedford MT and Leder P: Formin binding proteins bear WWP/WW domains that bind proline-rich peptides and functionally resemble SH3 domains. EMBO J 15: 1045-1054, 1996.

16. Ludes-Meyers JH, Kil H, Bednarek AK, Drake J, Bedford MT and Aldaz CM: WWOX binds the specific proline-rich ligand PPXY: Identification of candidate interacting proteins. Oncogene 23: 5049-5055, 2004.

17. Ferguson BW, Gao X, Zelazowski MJ, Lee J, Jeter CR, Abba MC and Aldaz CM: The cancer gene WWOX behaves as an inhibitor of SMAD3 transcriptional activity via direct binding. BMC Cancer 13: 593, 2013.

18. Ferguson BW, Gao X, Kil H, Lee J, Benavides F, Abba MC and Aldaz CM: Conditional Wwox deletion in mouse mammary gland by means of two cre recombinase approaches. PLoS One 7: e36618, 2012.

19. Abdeen SK, Salah Z, Khawaled S and Aqeilan RI: Characterization of WWOX inactivation in murine mammary gland development. J Cell Physiol 228: 1391-1396, 2013.

20. Bednarek AK, Keck-Waggoner CL, Daniel RL, Laflin KJ, Bergsagel PL, Kiguchi K, Brenner AJ and Aldaz CM: WWOX, the FRA16D gene, behaves as a suppressor of tumor growth. Cancer Res 61: 8068-8073, 2001.

21. Livak KJ and Schmittgen TD: Analysis of relative gene expression data using real-time quantitative PCR and the 2(-Delta Delta C(T)) method. Methods 25: 402-408, 2001.

22. Palma S, Raffa CI, Garcia-Fabiani MB, Ferretti VA, Zwenger A, Perez Verdera PV, Llontop A, Rojas Bilbao E, Cuartero V, Abba MC and Lacunza E: RHBDD2 overexpression promotes a chemoresistant and invasive phenotype to rectal cancer tumors via modulating UPR and focal adhesion genes. Biochim Biophys Acta 1866: 165810, 2020.

23. Bednarek AK, Laflin KJ, Daniel RL, Liao Q, Hawkins KA and Aldaz CM: WWOX, a novel WW domain-containing protein mapping to human chromosome 16q23.3-24.1, a region frequently affected in breast cancer. Cancer Res 60: 2140-2145, 2000.

24. Chammas R, Taverna D, Cella N, Santos C and Hynes NE: Laminin and tenascin assembly and expression regulate HC11 mouse mammary cell differentiation. J Cell Sci 107: 1031-1040, 1994.

25. Shiu RP and Paterson JA: Alteration of cell shape, adhesion, and lipid accumulation in human breast cancer cells (T-47D) by human prolactin and growth hormone. Cancer Res 44: 1178-1186, 1984.

26. Chambon M, Rochefort H, Vial HJ and Chalbos D: Progestins and androgens stimulate lipid accumulation in T47D breast cancer cells via their own receptors. J Steroid Biochem 33: 915-922, 1989.

27. Ronen D, Altstock RT, Firon M, Mittelman L, Sobe T, Resau JH, Vande Woude GF and Tsarfaty I: Met-HGF/SF mediates growth arrest and differentiation in T47D breast cancer cells. Cell Growth Differ 10: 131-140, 1999.

28. Canzoneri R, Rabassa ME, Gurruchaga A, Ferretti V, Palma S, Isla-Larrain M, Croce MV, Lacunza E and Abba MC: Alternative splicing variant of RHBDD2 is associated with cell stress response and breast cancer progression. Oncol Rep 40: 909-915, 2018.

29. Bonin F, Taouis K, Azorin P, Petitalot A, Tariq Z, Nola S, Bouteille N, Tury S, Vacher S, Bièche I, *et al*: VOPP1 promotes breast tumorigenesis by interacting with the tumor suppressor WWOX. BMC Biol 16: 109, 2018.

30. Fontes-Sousa M, Amorim M, Salta S, Palma De Sousa S, Henrique R and Jerónimo C: Predicting resistance to endocrine therapy in breast cancer: It's time for epigenetic biomarkers (Review). Oncol Rep 41: 1431-1438, 2019.

31. Nunez MI, Ludes-Meyers J, Abba MC, Kil H, Abbey NW, Page RE, Sahin A, Klein-Szanto AJ and Aldaz CM: Frequent loss of WWOX expression in breast cancer: Correlation with estrogen receptor status. Breast Cancer Res Treat 89: 99-105, 2005.